[redacted]

Coordinated Science Laboratory

UNIVERSITY OF ILLINOIS - URBANA, ILLINOIS

AN ALGEBRAIC STUDY OF SHOCK STRUCTURE

B. L. Hicks and S. M. Yen

REPORT R-244 FEBRUARY, 1965

This work was supported wholly by the Joint Services Electronics Programs (U.S. Army, U.S. Navy, and U.S. Air Force) under Contract No. DA 28 043 AMC 00073(E).

AN ALGEBRAIC STUDY OF SHOCK STRUCTURE

B. L. Hicks and S. M. Yen

Abstract

Far up- and downstream of a shock front the structure of a shock must conform to the Navier-Stokes equations. At these boundaries, therefore, the viscosity coefficient $\tilde{\mu}$ and Prandtl number $\tilde{Pr}$ must have values appropriate to the medium and the conditions there. For a monatomic gas, $\tilde{Pr}$ must equal 8/9, and the derivatives of $t_\perp$ (the lateral temperature) and of dn/dx (the density gradient) are calculable. We can use these conditions to test the accuracy of various theoretical shock structures proposed and to find approximate macroscopic properties of shock structures for any monatomic gas without solving the Boltzmann equation. We have developed the corresponding first order theory in algebraic form by modifying the Mott-Smith expressions for $t_\perp$ and dn/dx in a simple way such that the modified functions will satisfy the auxiliary conditions and will thus agree with the known transport characteristics of monatomic gases. By using the number density n as the independent variable, we are able to find the macroscopic shock structure on the basis of given asymptotic values of $\tilde{Pr}$ alone, while the spatial distribution of properties depends on both $\tilde{Pr}$ and $\tilde{\mu}$.

Comparisons are presented of the shock structures for monatomic gases calculated according to the first order algebraic theory, Mott-Smith, and Navier-Stokes. The first order theory reproduces the Navier-Stokes results in the low Mach number range and supplies a simple representation of the Navier-Stokes model. At high Mach number, the correction of the

properties to the Mott-Smith model amount to at most less than 20 per cent of stress τ/p_1 or of the heat flux q. The shock thickness is much smaller than Camac's experimental value for argon.

A second order calculation may be made by including as an additional condition the matching of any experimentally determined shock thickness. As an example calculations are given for argon.

I. Introduction

In studies of shock structure it is advantageous to use the number density n as the independent variable in place of the distance variable x. The velocity distribution function, each moment of it that is of interest, and the density gradient dn/dx are then to be regarded as functions of n rather than of x. If needed, the x dependence of the various quantities can be recovered by integration.

The Mott-Smith distribution function for a shock wave[1] implies that the moments are linear functions of n and that dn/dx has a particular quadratic form in n. In this paper we shall use n as an independent variable to study other characteristics of the Mott-Smith model and to derive asymptotic tests that can be applied to any proposed solution of the Boltzmann equation for a shock wave. The asymptotic tests we shall propose are based upon the arguments that there are two near-equilibrium regions, far up- and downstream from the shock front; and that any theoretical shock must conform to the Navier-Stokes equation in these two regions in that the transport coefficients and their derivatives must have values appropriate to the medium in these near-equilibrium conditions. We shall use the tests in making first order improvement of the Mott-Smith model for a monatomic gas by purely algebraic modification of his theory which then leads to the correct asymptotic transport coefficients.

Results of the first order theory have been obtained for elastic sphere molecules and for argon. We have also developed a second order

---

[1] H. M. Mott-Smith, Phys. Rev. 82, 885 (1951).

theory for argon by matching the experimental shock thickness as well as the asymptotic transport coefficients.

II. Asymptotic Tests of Shock Structure

Near the cold or hot side of a shock wave the gas is almost in equilibrium, and the usual transport equations hold

$$\tau = \tilde{\mu} \frac{du}{dx} \tag{1}$$

$$-Q = k \frac{dt}{dx} \tag{2}$$

in which $\tilde{\mu} = \frac{4}{3}\mu$ and the values of the shear viscosity μ and of the coefficient of heat conductivity k are known from kinetic theory for a monatomic gas. One can show by using the standard definitions of the flux of macroscopic properties in terms of velocity moments, that the stress τ and a non-dimensional heat flux q in these equations have the form

$$\begin{aligned} \tau/p_1 &= \left\{ \frac{1}{3} \int m(v_\perp^2 - 2v_x^2) f(\vec{v}) d\vec{v} \right\} / p_1 \\ &= \frac{2}{3} n(t_\perp - t_x) \end{aligned} \tag{3}$$

$$\begin{aligned} q = \frac{2Q}{p_1 u_1} &= 2\left\{ \int m v_x \frac{v^2}{2} f(\vec{v}) d\vec{v} \right\} / p_1 u_1 \\ &= \frac{5}{3}(3 + M_1^2) - 3t_x - 2t_\perp - \underset{\sim}{t} \end{aligned} \tag{4}$$

We are using as units of temperature and number density the upstream values of these variables. u is the mass velocity. $v = (v_x, v_\perp)$ is the peculiar velocity. $f(\vec{v})$ is the velocity distribution function. M_1 and p_1 are the upstream values of the Mach number and pressure. The temperatures t_x, $t_\perp$, and $\underset{\sim}{t}$ refer to the translational temperatures associated with

longitudinal and lateral thermal velocities and with the mass velocity of the gas respectively. The temperatures t_x and $\underset{\sim}{t}$, as functions of n, can be determined from the conservation equations alone and are given by

$$t_x = (4 - n_2)^{-1} n^{-2} [4(n_2 + 1)n - 5n_2] \tag{5}$$

$$\underset{\sim}{t} = 5n_2(4 - n_2)^{-1} n^{-2} \tag{6}$$

The downstream value of the number density n_2 depends only on M_1

$$n_2 = \frac{4M_1^2}{3 + M_1^2} \tag{7}$$

If the transverse temperature $t_\perp$ is known as a function of the number density n for a given Mach number M_1, then, according to Equations (3) and (4), the fluxes τ/p_1 and q will also be known functions of n. The same may be said for the transport coefficients $\tilde{\mu}$ and k if the function dn/dx is known and the two transport coefficients are defined within the shock by Equations (1) and (2).

A proposed solution of the Boltzmann equation for a shock wave may be put in the form of a specification of the velocity distribution function, which we may write for our purposes as $f(\vec{v},n)$, and of the gradient function dn/dx. From f we can calculate the moment $(nt_\perp)$. Knowing $t_\perp$ we can calculate $\tilde{\mu}$ and k throughout the shock wave and in particular at the cold and hot sides. If these values are correct at these boundaries we may say that the proposed solution satisfies the Boltzmann equation there in the sense that it predicts the same values of these coefficients as would an exact solution of the Boltzmann equation. In developing and using this

test it is convenient to use $\widetilde{Pr}$ and σ rather than the two transport coefficients, where the Prandtl number

$$\widetilde{Pr} = \widetilde{\mu}\, C_p/k = 3M_1^{-2}\, n^2 \left(\frac{dt}{dn}\right) \frac{(\tau/p_1)}{(q)} \tag{8}$$

and the quantity

$$\sigma = \mu/\mu_1 = - \frac{3}{16(0.499)} \sqrt{\frac{3\pi}{5}}\; n^2 M_1^{-1}\; \frac{(\tau/p_1)}{(dn/dx)} \tag{9}$$

indicates the departure of the viscosity from its value μ_1 at the cold side. $\widetilde{Pr}$ has the value 8/9 for any monatomic gas. The viscosity at the cold side $\mu_1 = 0.499\, \rho_1\, \bar{v}_1\, \lambda_1$ where λ_1 = mean free path at the cold side.

The dimensionless temperature variables are related by the equation

$$t = (t_x + 2t_\perp)/3 \tag{10}$$

III. Application to the Mott-Smith Model

Straightforward calculations based on the Mott-Smith form[1] of velocity distribution function in a shock wave lead to the following expressions:

$$(t_\perp)_{MS} = \left[1 + \frac{t_2 - 1}{n_2 - 1}\,(n-1)\right] + \frac{(n-1)(n_2-n)}{n^2} \left[\frac{1 + n_2}{n_2(4-n_2)}\right] \tag{11}$$

$$\left(\frac{dn}{dx}\right)_{MS} = (n - 1)\,(n_2 - n) \left[\frac{B}{n_2 - 1}\right] \tag{12}$$

where B = a constant depending on the molecular velocity function chosen for the transport equation. From $t_\perp$ (Equation (11)) we can find expressions for all of the significant macroscopic properties that are functions of

true velocity moments. We give the following expressions for τ/p_1 and q as examples:

$$(\tau/p_1)_{MS} = -\frac{10}{3}(4 - n_2)^{-1} n^{-1} (n - 1)(n_2 - n) \tag{13}$$

$$(q)_{MS} = -10(4 - n_2)^{-1} n^{-2} (n - 1)(n_2 - n) \tag{14}$$

The x dependence of these properties can be determined, if needed, from Equation (12). Equations (11) - (14) are used in determining the transport parameters $\tilde{Pr}$ and σ:

$$(\tilde{Pr})_{MS} = \frac{2}{9} n_2^{-1} [5n_2 - (n_2 + 1) n] \tag{15}$$

$$(\sigma)_{MS} = \frac{\sqrt{3\pi/5}}{8(0.499)} B^{-1} M_1^{-1} (n_2 - 1)(4 - n_2) \left\{5n - \frac{(1+n_2)}{n_2} n^2\right\} \tag{16}$$

As noted before $\tilde{Pr}$ depends only on $t_\perp$ and is <u>therefore independent of dn/dx</u>.

From Equations (7) and (15) we find that the Prandtl number on either side of a Mott-Smith shock wave depends only on M_1 and can not exceed the value 5/6. It vanishes on the hot side of the shock wave as $M_1 \to \infty$ (or as $n_2 \to 4$). On the other hand, σ has a wide range of values at the cold side and is smaller than the correct asymptotic value at the hot side. We shall show in the next section how these deficiencies of the Mott-Smith model can be overcome.

IV. Algebraic Modification of the Mott-Smith Model

On the basis of our earlier discussion, we see that two Mott-Smith functions available for modification are the transverse temperature $t_\perp$ and the gradient function dn/dx. Modification of these functions will, of course, place restrictions upon the form of the velocity distribution function itself, and these functions should correspond to a steadily decreasing Boltzmann flux. We shall not discuss these restriction further here, but we shall use the fact that the modifications must be of such a nature that they vanish on the boundaries far upstream and downstream.

As an example of our algebraic modifications we first develop a first order theory by making a modification of the Mott-Smith $t_\perp(n)$:

$$t_\perp = (t_\perp)_{MS} + t_\perp^* \tag{17}$$

where

$$t_\perp^* = \frac{(n-1)(n_2-n)}{n^2}\left[C_o n + C_1 n^2\right] \tag{18}$$

which corresponds to

$$\tau/p_1 = (\tau/p_1)_{MS} + 2nt^*/3 \tag{19}$$

$$q = (q)_{MS} - 2t^* \tag{20}$$

$$\tilde{Pr} = M_1^{-2}\, n^3 \left[\frac{1-\xi}{1+\xi}\right]\left(\frac{dt}{dn}\right) \tag{21}$$

with

$$\xi = n(C_o' + C_1' n) = \frac{1}{5}(4 - n_2)n(C_o + C_1 n) \tag{22}$$

We then also modify the form of the Mott-Smith dn/dx:

$$dn/dx = (n - 1)\ (n_2 - n)\ (A_o + A_1 n) \tag{23}$$

which corresponds to

$$\sigma = \frac{\sqrt{15\pi}}{8(0.499)}\ (4 - n_2)^{-1}\ M_1^{-1}\ n\ \frac{(1 - \xi)}{(A_o + A_1 n)} \tag{24}$$

where the unit of x is $\lambda_1/\sqrt{2}$ and λ_1 is the upstream mean free path. C_o' and C_1' are more convenient to use than C_o and C_1 because each of the former remains finite as $M_1 \to \infty$. A similar algebraic correction factor, which we have not investigated, would involve larger negative powers of n instead of larger positive powers.

The four constants C_o', C_1', A_o, A_1 are to be determined for each Mach number by requiring that the modified model yields the correct values of $\tilde{Pr}$ and $\tilde{\mu}$ at each of the two boundaries of the shock wave. The advantage of using the Prandtl number in place of k is now clear: Equation (21) involves only C_o' and C_1' but not A_o and A_1, corresponding to the fact that $\tilde{Pr}$ is related to dt/dn but not to dn/dx and dt/dx separately.

Examination of Equation (21) shows that it yields at each boundary a quadratic equation in ξ, and that for any Mach number the roots of the quadratic are real. Only one root for each boundary gives results on macroscopic properties in agreement with Navier-Stokes for low Mach numbers. We discard the other roots and call the surviving roots ξ_1 and ξ_2.

Values of C_o', C_1' and of ξ_1, ξ_2 calculated from the two quadratics are listed in Table I for the complete range of Mach number from one to infinity. Corresponding values of A_o and A_1 derived from Equation (24) for the case of

elastic sphere are also listed in Table I.

Table I. Parameters of the First Order Algebraic Theory

Monatomic Gases

M_1	C_o'	C_1'	ξ_1	ξ_2	A_o	A_1
					(Elastic Sphere)	
1.00	-0.1924	0.04956	-0.1428	-0.1428	0.1650	0.4901
1.40	-0.1483	0.02923	-0.1191	-0.1614	0.1861	0.3821
2.00	-0.1151	0.01735	-0.0978	-0.1725	0.2536	0.2970
3.00	-0.0934	0.01127	-0.0821	-0.1787	0.4012	0.2191
5.00	-0.0810	0.00840	-0.0726	-0.1820	0.7483	0.1124
10.00	-0.0754	0.00727	-0.0682	-0.1834	1.7084	-0.1317
∞	-0.0736	0.00690	-0.0667	-0.1838	∞	$-\infty$

V. Discussion

We remark first that ξ_1 and ξ_2 are negative for all M_1, which implies that the values of $|q|$ and of $t_\perp$ and t are smaller than in the Mott-Smith model and that the values of $|\tau|$ are greater. Second, we notice that the largest values of ξ_1 and ξ_2 occur at the hot side of the shock and that these values are never greater than 0.2. Thus the correction of τ/p_1 or of q needed in the Mott-Smith theory to give correct up- and downstream values of $\tilde{Pr}$ are never larger than 20 percent.

From the values of the two parameters C_o' and C_1' we can determine p/p_1, t, M and $\tilde{Pr}$ throughout the shock. We have seen that knowledge of $t_\perp$ implies knowledge of each of these functions so that they are not, therefore, independent of one another. It is nevertheless instructive to look at the characteristics of several of them. We have chosen t, q, τ/p_1 and $\tilde{Pr}$ for more detailed examination. The study of $\tilde{Pr}$ allows a rather

dramatic comparison to be made among the results of the algebraic and Mott-Smith theories. When A_o and A_1 are also known we can of course calculate dn/dx and σ.

As an appropriate measure of position within the shock we shall use

$$\hat{n} = \frac{n-1}{n_2-1} \tag{25}$$

which measures the fraction of the total distance through the shock. To make our results easily comparable with other studies we shall use

$$\eta(n,M_1) = \frac{\sqrt{2}}{n_2-1}\left(\frac{dn}{dx}\right) = \sqrt{2}\,\frac{d\hat{n}}{dx} \tag{26}$$

in place of dn/dx. η is thus the fractional density gradient in units of upstream reciprocal mean free path, and its maximum value for each Mach number is the usual reciprocal shock thickness.

One virtue of the algebraic and of the Mott-Smith theories is the ease with which we can determine the behavior of the various functions as $M_1 \to \infty$. Thus we can easily show that the following quantities remain finite (in each theory) as $M_1 \to \infty$: $M_1^{-2}t$, $M_1^{-2}p$, $M_1^{-2}\tau/p_1$, $M_1^{-2}q$, $M_1^{-1}dn/dx$; $\widetilde{Pr}$, and σ. Putting these ideas together we choose to use $M_1^{-2}t$, $M_1^{-2}\tau/p_1$, and $M_1^{-2}q$ in place of t, τ/p_1 and q respectively in exhibiting the principal results on macroscopic properties of the algebraic theory.

We shall in this paper compare the results of the algebraic theory with those from Navier-Stokes and Mott-Smith. The Navier-Stokes results were obtained by H. J. Schmidt.[2]

---

[2] H. J. Schmidt, M. S. Thesis, Aero. and Astro. Engr. Dept., Univ. of Ill., 1964.

1. Macroscopic Properties

It is well-known that the asymptotic properties of a Navier-Stokes wave can be obtained from the integral curve in the u-t (velocity-temperature) plane. The integral curve has a singularity at each end point[3] (a saddle point on the hot side and an improper node at the cold side). The values of the derivatives at both sides of the shock may be obtained algebraically. The derivative du/dt is related to dt/dn used here by the following expression

$$\left(1 + \frac{5}{3} M_1^2\right) \frac{du}{dt} = - \frac{(1 + 5M_1^2/3)}{M_1^2} \frac{1}{n^2} \left[M_1^{-2} \frac{dt}{dn} \right]^{-1} \qquad (27)$$

We found that the asymptotic (boundary) values of $M_1^{-2}(dt/dn)$ of the first order theory agree with the corresponding Navier-Stokes values in the entire range of M_1. (We note also that at the hot side of the shock $M_1^{-2}(dt/dn)$ has a finite limit as $M_1 \to \infty$ as compared to zero for the Mott-Smith case.) The agreement of dt/dn with Navier-Stokes values implies that the asymptotic derivatives of all the macroscopic properties of first order theory that are determined by $t_\perp$ also match the Navier-Stokes derivatives.

The distribution of properties within the shock are illustrated in Figures 1, 2, 3, and 4 in which $\tilde{Pr}$, $M_1^{-2}t$, $M_1^{-2}\tau/p_1$, and $M_1^{-2}q$ respectively are plotted.

The value of the Prandtl number $\tilde{Pr}$ (Figure 1) in the Mott-Smith model is very much too small on the hot side of the shocks for large M_1. The algebraic theory of course yields the correct values of $\tilde{Pr}$ at both boundaries for all values of M_1. It is noted that the curves of $\tilde{Pr}$ vs. $\hat{n}$ are very

[3] R. von Mises, J. Aero. Sci., 17, 551 (1950).

nearly symmetrical for the algebraic theory. It should be remembered that $\tilde{Pr}$ has been defined within the shock by Equation (8). For a monatomic Navier-Stokes gas, $\tilde{Pr}$ has the constant value of 8/9 throughout the shock.

The algebraic theory reproduces well the Navier-Stokes values of $M_1^{-2}t$ inside the shock wave up to M_1 of 1.6, and τ/p_1 and q up to M_1 of 1.4. For higher M_1, the results of algebraic theory fall between those of Navier-Stokes and those of Mott-Smith but lie closer to the Navier-Stokes values. In fact, appreciable deviation from the Navier-Stokes results occurs only in the "center" of the shock. The degree of asymmetry of all three profiles is about the same for all the profiles for all three cases.

2. dn/dx and Shock Thickness

The gradient dn/dx depends on both transport coefficients. To determine it we need, therefore, all four coefficients of our algebraic theory (C_o, C_1, A_o, and A_1). The values of dn/dx have been calculated for the following three power laws for viscosity ($\mu \sim t^{\nu}$):

$$\nu = 0.5 \text{ (elastic sphere)}, 0.75, 0.816.$$

The last two cases are useful in comparing the results on shock thickness with experimental values of argon. The distribution of $\sigma t^{-1/2}$ within the shock for the elastic sphere model is plotted in Figure 5. As M_1 increase the $\sigma t^{-1/2}$ vs $\hat{n}$ curve becomes more asymmetrical with the position of minimum shifting toward the cold side. For Navier-Stokes, the $\sigma t^{-1/2}$ curve is a straight line. The values of B used to calculate the Mott-Smith curves correspond to the molecular velocity function of (axial velocity)^2.

The reduced gradient function $d\hat{n}/dx$ for the elastic sphere model is plotted in Figure 6. Both reciprocal shock thickness (equal to the maximum ordinate) and asymmetry can be determined from these curves very easily. The reciprocal shock thickness calculated from our first order algebraic theory agree well with the Navier-Stokes values for values of M_1 up to 1.6 (as shown in Figure 7) but at higher M_1 the first order theory gives much higher values (as shown in Figure 8).

Another use of $d\hat{n}/dx$ would be to find the spatial distribution of the macroscopic properties. Since this can be done in a straightforward way, we will not discuss it further.

3. Comparison With Experimental Results and Second Order Theory

The values of $d\hat{n}/dx$ obtained for values of the viscosity parameter $\nu = .75$ and $\nu = 0.816$ are useful in comparing with the reciprocal shock thickness determined by experiments for argon. In Figure 9 reciprocal shock thickness is plotted vs M_1. Camac's data[4] are also included. Just as in the case of elastic sphere ($\nu = 0.5$), the reciprocal shock thickness is much too large in the high M_1 ranges.

We can use such a discrepancy with his experimental results in making a second order calculation. Thus we add a term in the correction polynomial of dn/dx (see Equation 23) as follows:

$$dn/dx = (n - 1)\,(n_2 - n)\,(A_o + A_1 n + A_2 n^2). \qquad (28)$$

---

[4] M. Camac, Research Report 172, AVCO-Everett Research Laboratory, Dec. 1963.

The three coefficients, A_o, A_1, and A_2 may be determined by using Camac's (or any other) experimentally determined maximum value of dn/dx in addition to asymptotic values of σ as used in the first order theory. Correct values of dn/dx in the up- and downstream near-equilibrium regions are, therefore, also obtained in such a calculation. Furthermore, the expression for $\tilde{Pr}$ remains the same, and the profiles of macroscopic properties determined by $t_\perp$ are the same with respect to n as those of the first order theory.

We have made a second order calculation for $M_1 = 3$ for argon ($\nu = 0.75$) by matching $(d\hat{n}/dx)_{max}$ at $\hat{n} = 1/2$ to Camac's value. The coefficients obtained are: $A_o = 1.523$, $A_1 = -1.228$, $A_2 = 0.3250$. (The coefficients for the first order theory for the same M_1 and ν are: $A_o = 0.5479$, $A_1 = 0.07234$.) The corresponding η curve which is plotted in Figure 10 exhibits a flat region near the "center" in the shock and a corresponding region of large curvature on either side of the "center". The second order theory thus illustrates the general shape which the η vs $\hat{n}$ curve must have if it is to reproduce both the Navier-Stokes behavior in the near-equilibrium regions and Camac's experimental value of the ordinate at the center of the profile. More complete theory is needed to determine whether the curve should be more or less asymmetric than the one shown.

ACKNOWLEDGMENT

We are indebted to Dr. H. M. Mott-Smith for several helpful comments during the preparation of this report.

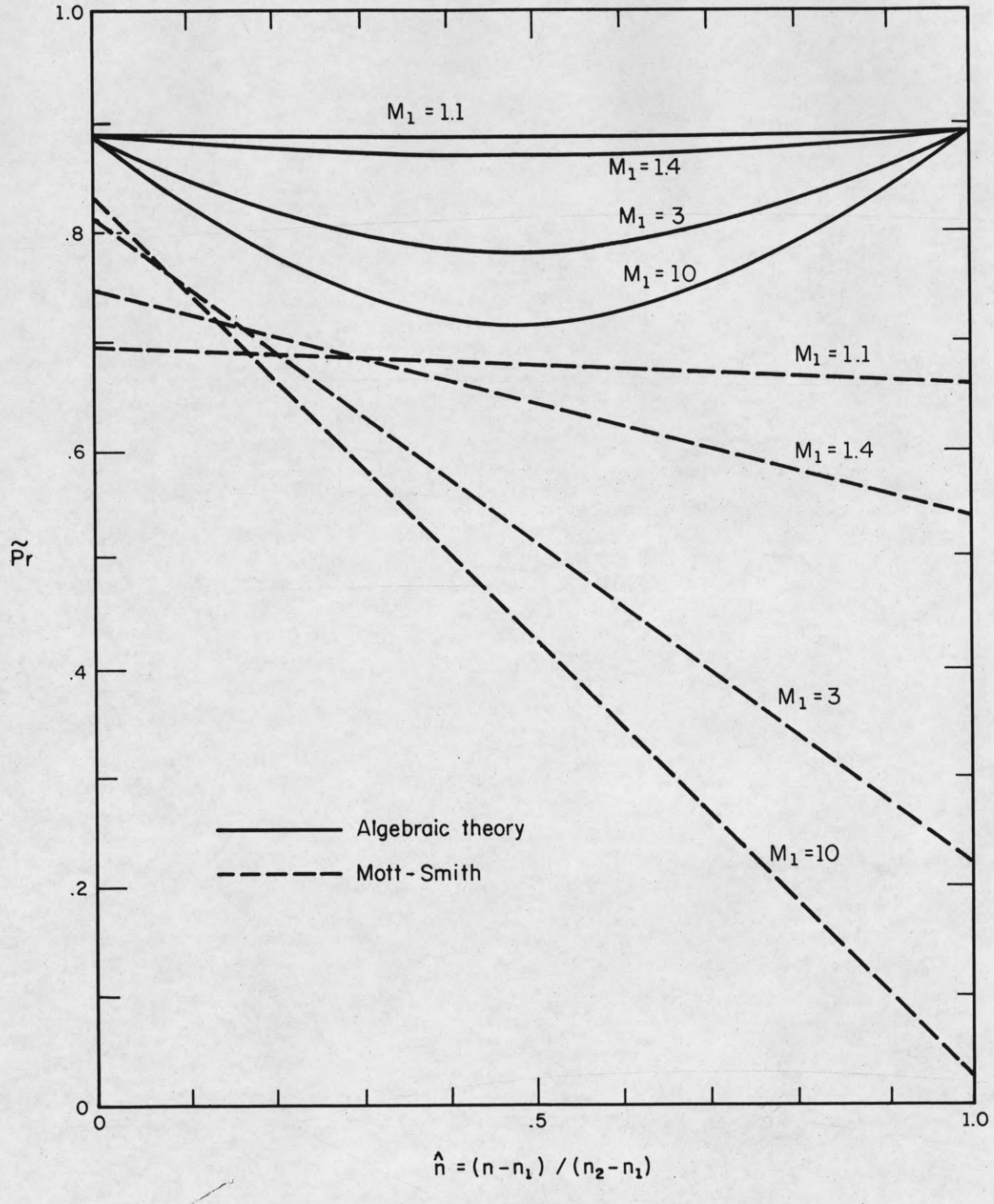

Fig. 1 Variation of Prandtl number $\tilde{Pr}$ with reduced number density $\hat{n}$.

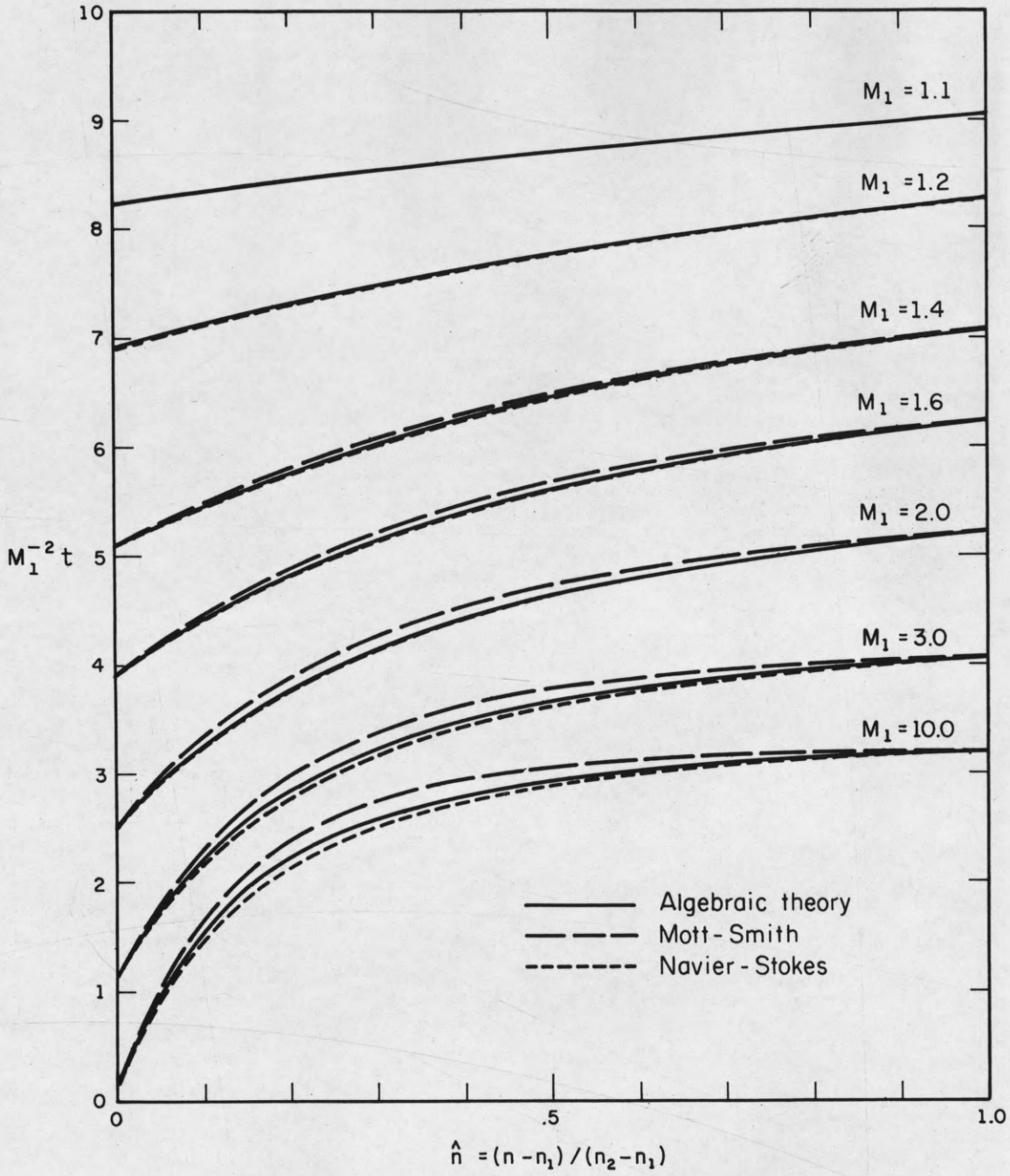

Fig. 2 Variation of reduced temperature $M_1^{-2}t$ with reduced number density $\hat{n}$.

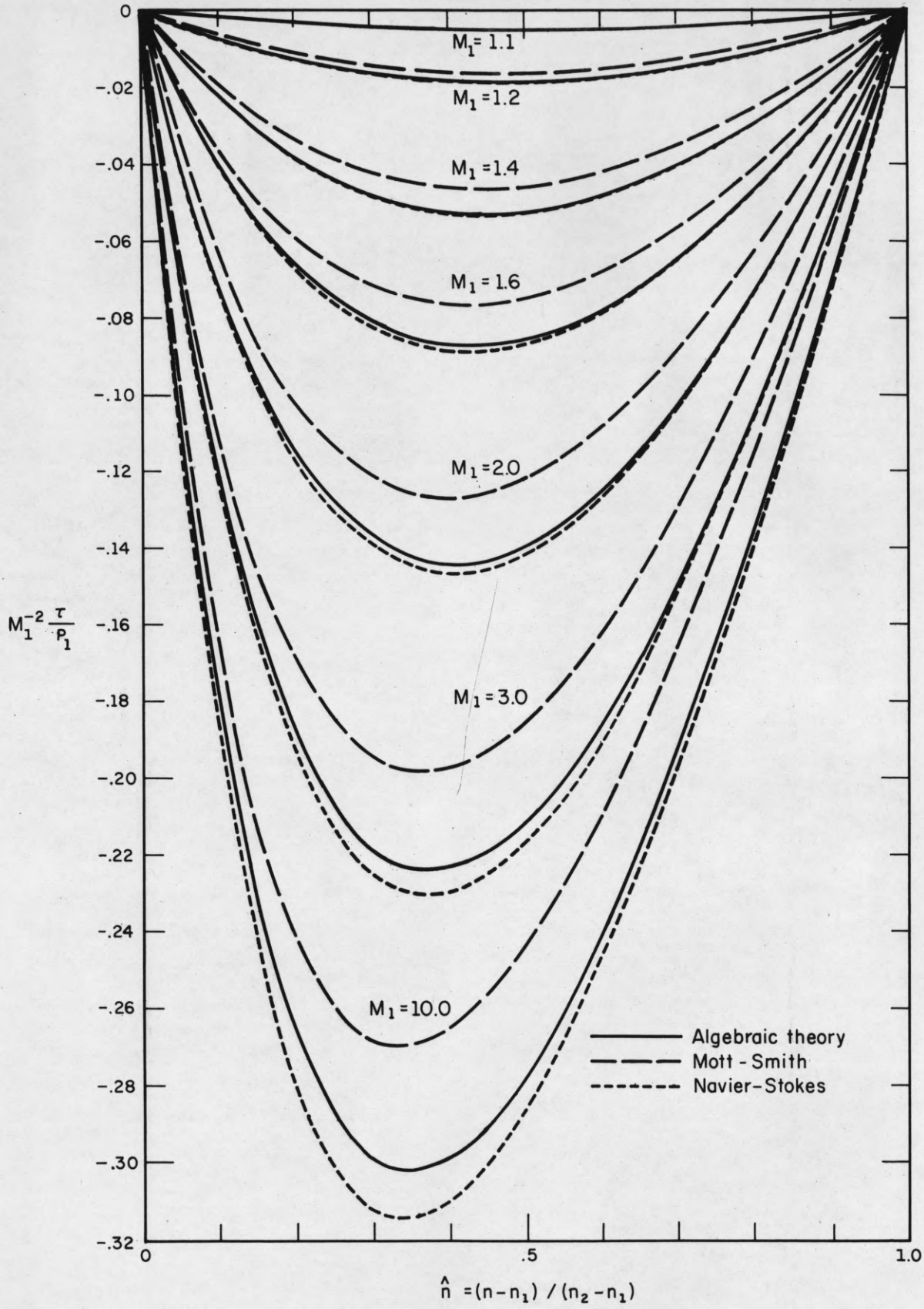

Fig. 3 Variation of reduced stress $M_1^{-2}\tau/p_1$ with reduced number density $\hat{n}$.

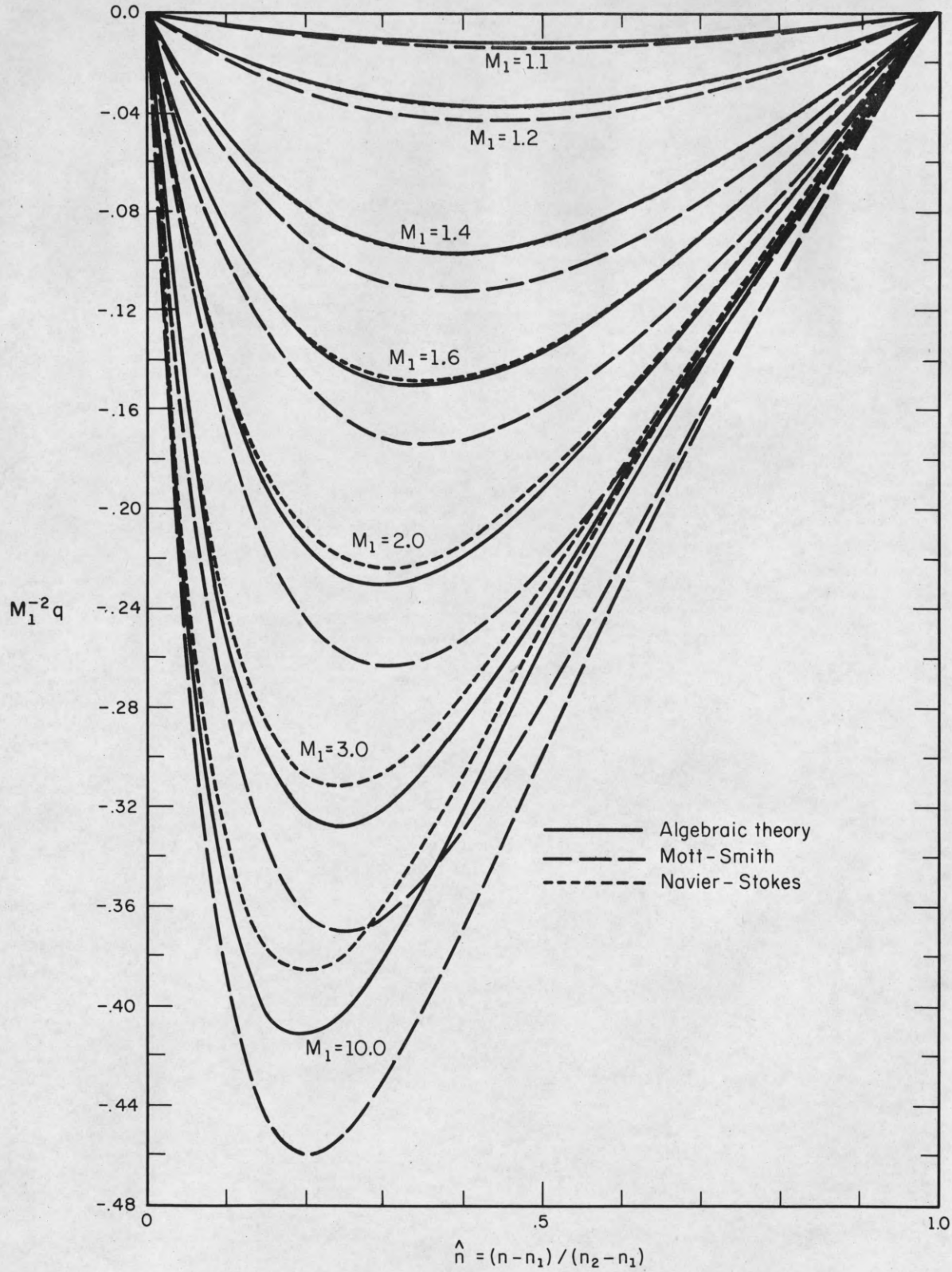

Fig. 4 Variation of reduced heat flux $M_1^{-2}q$ with reduced number density $\hat{n}$.

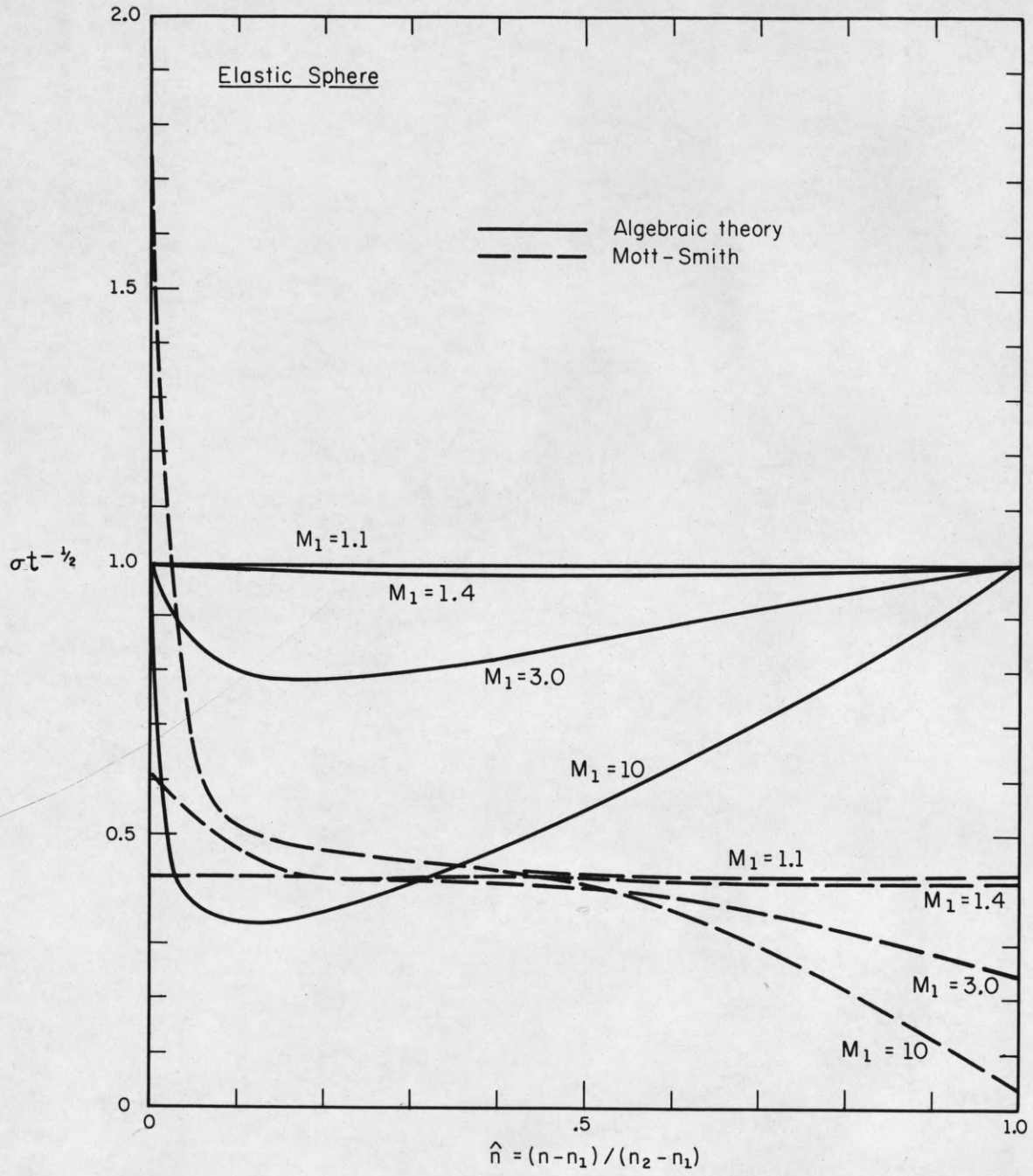

Fig. 5 Variation of viscosity parameter $\sigma t^{-1/2}$ with reduced number density $\hat{n}$.

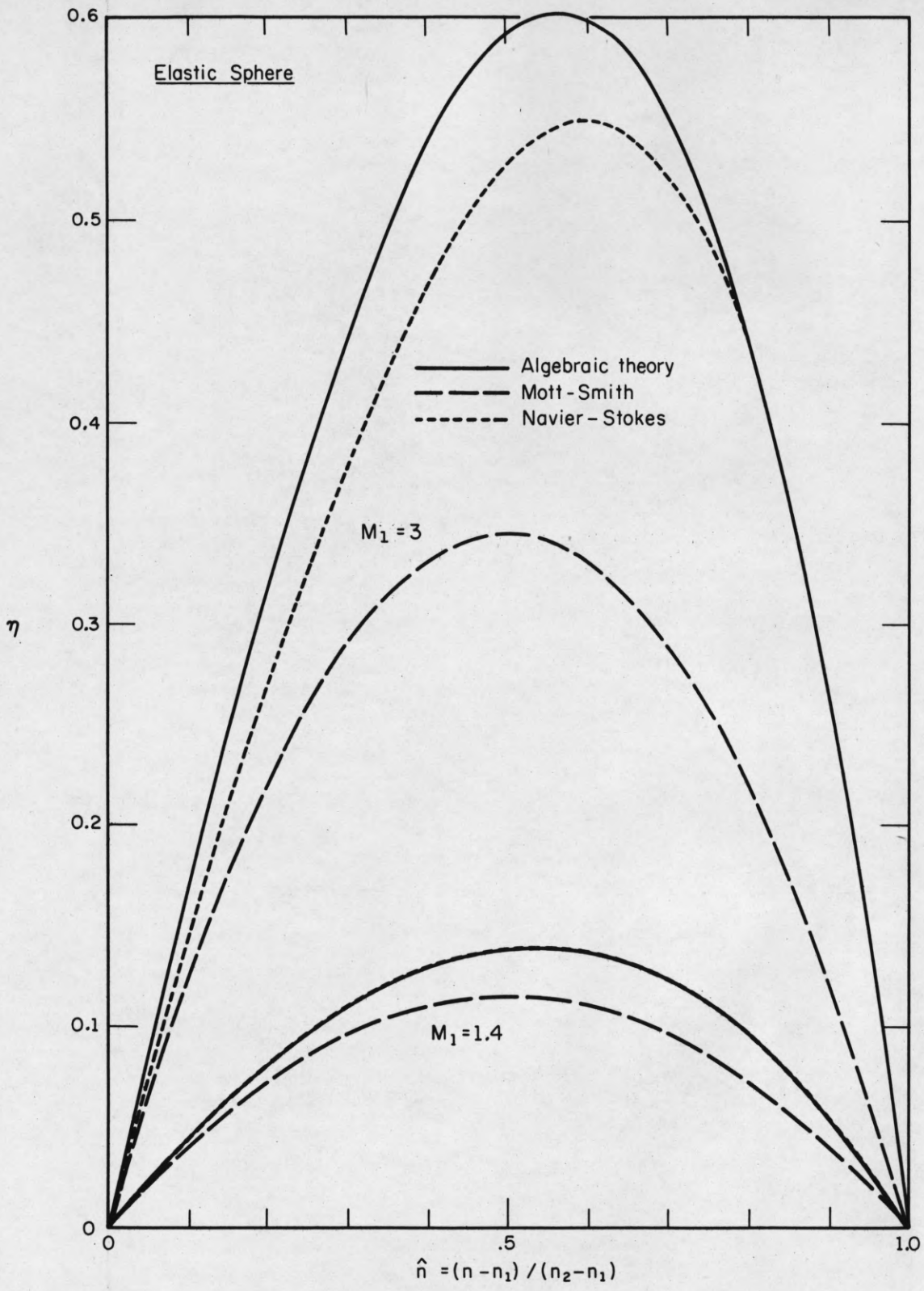

Fig. 6 Variation of fractional density gradient η with reduced number density $\hat{n}$.

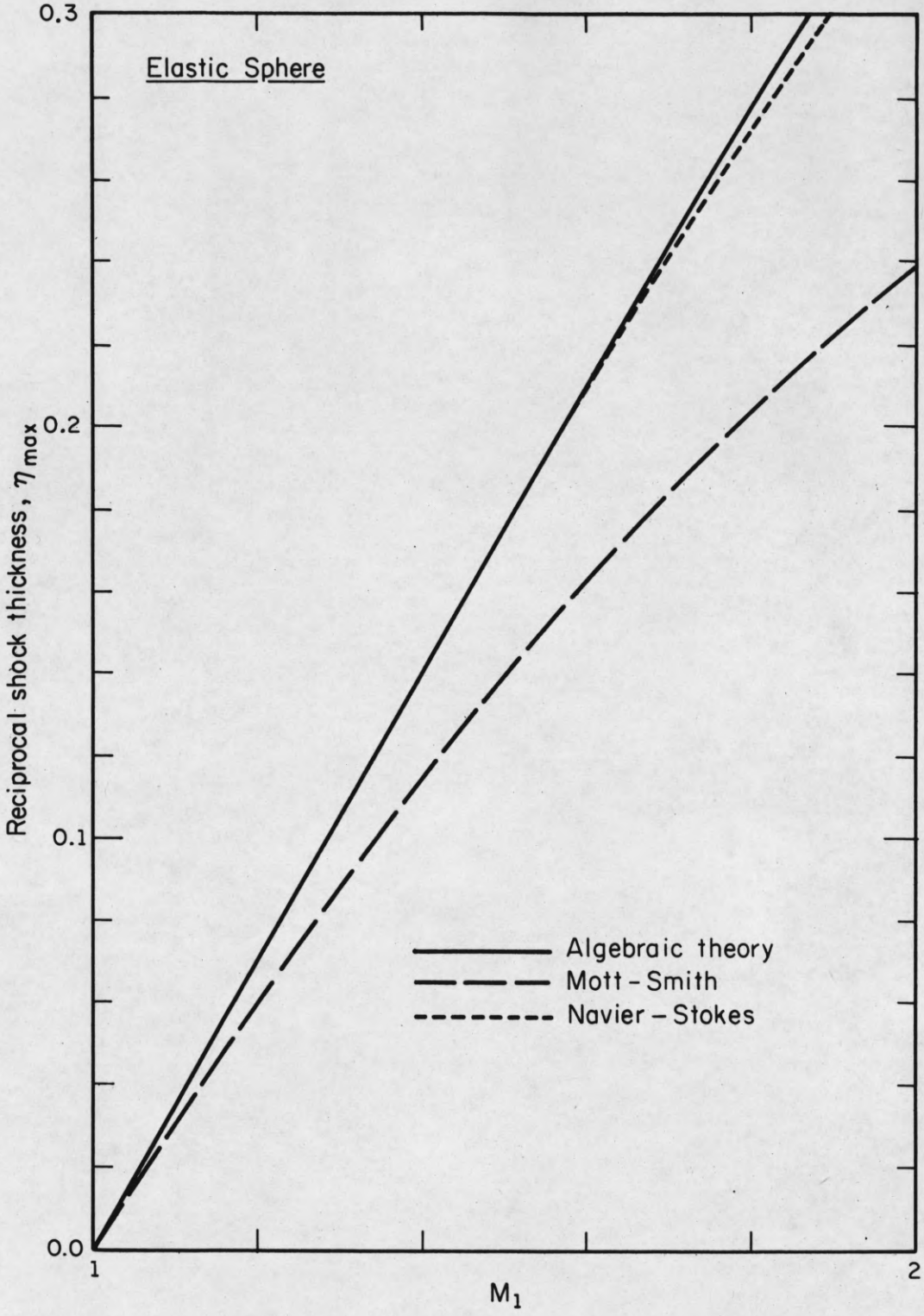

Fig. 7 Variation of theoretical reciprocal shock thickness η_{max} with upstream Mach number M_1 for weak shocks.

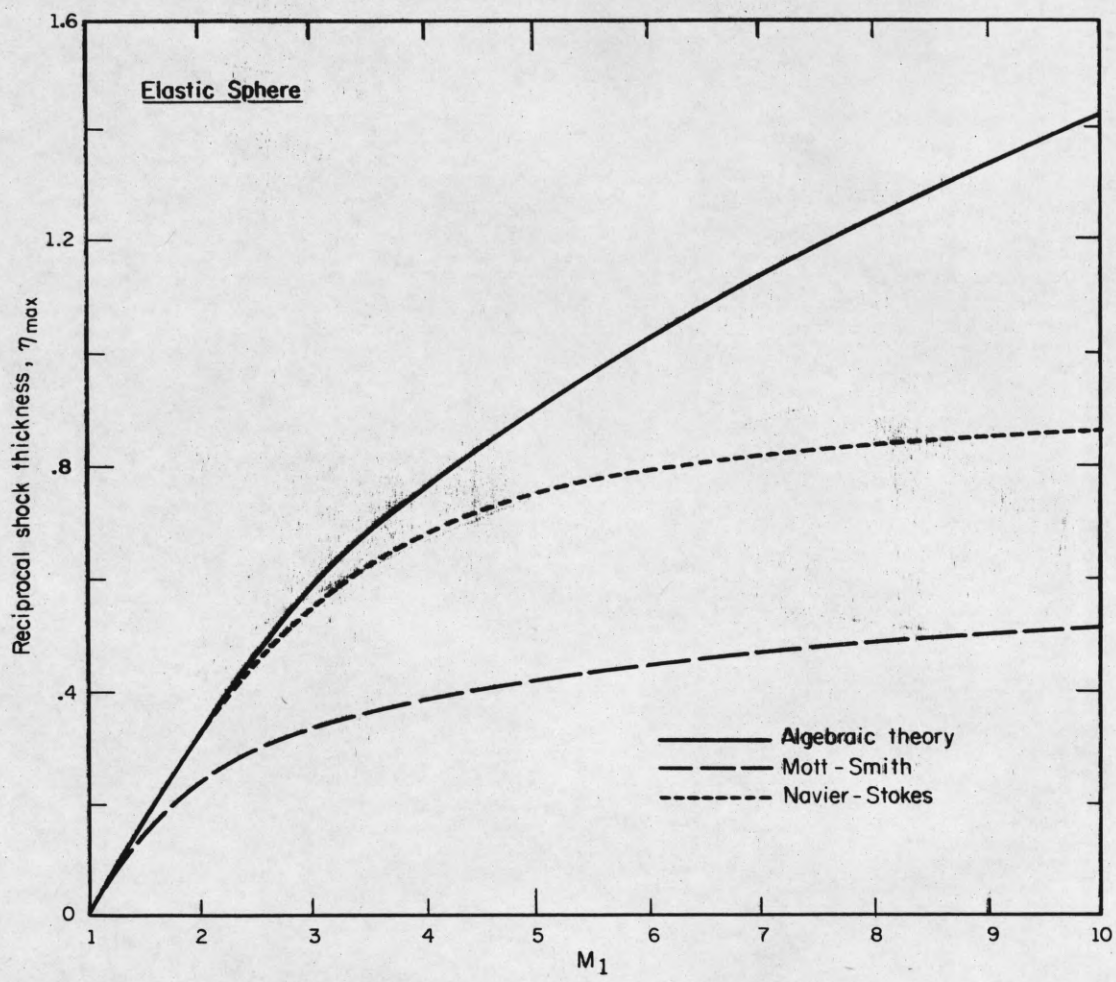

Fig. 8 Variation of theoretical reciprocal shock thickness η_{max} with upstream Mach number M_1.

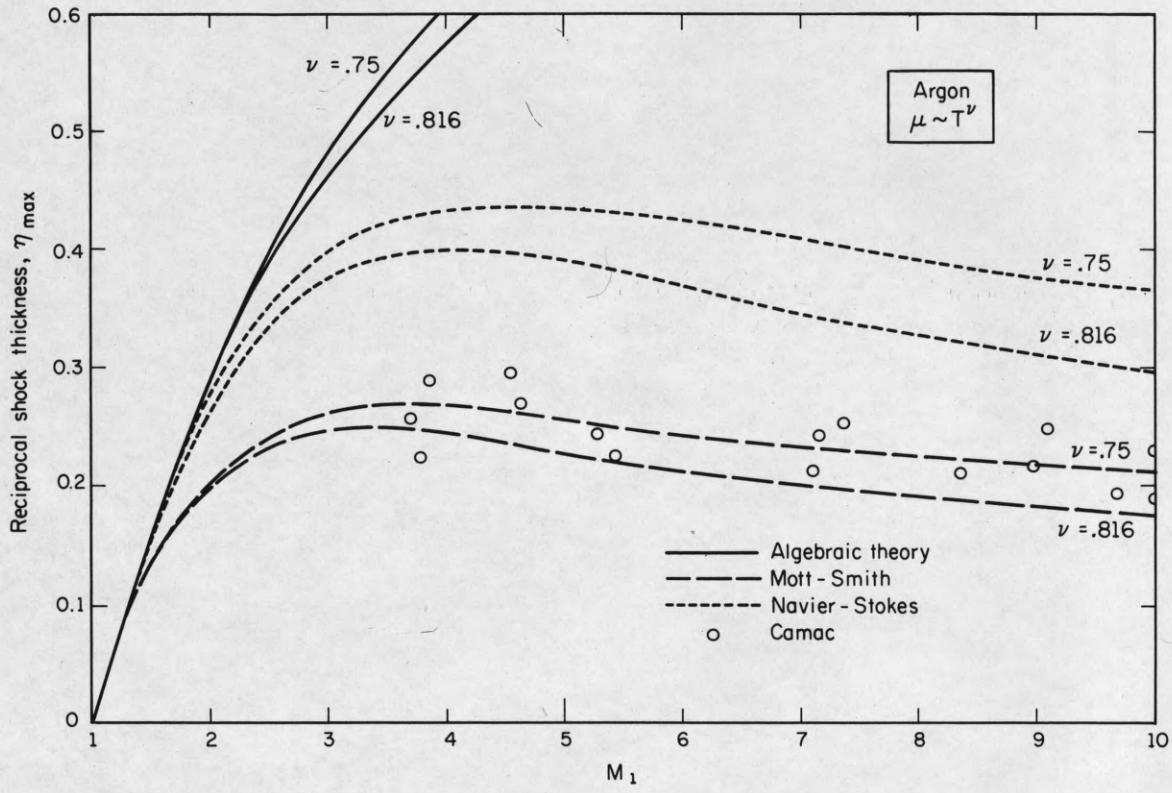

Fig. 9 Comparison of theoretical and experimental reciprocal shock thickness for argon.

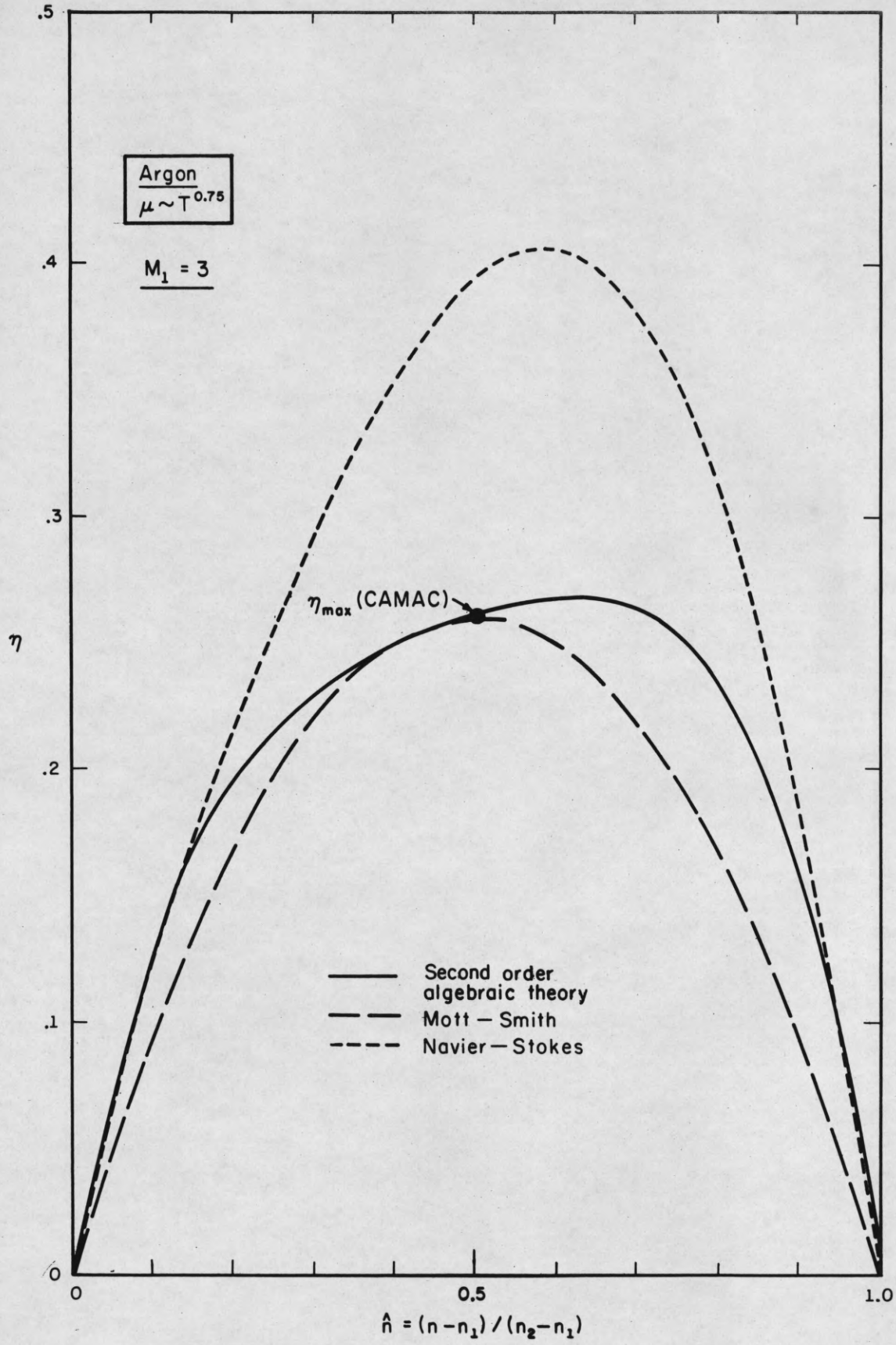

Fig. 10 Variation of fractional density gradient η with reduced number density $\hat{n}$ for argon for $M_1 = 3$. Comparison of second order algebraic theory with other values.

Distribution list as of September 1, 1964

1 Director
Air University Library
Maxwell Air Force Base, Alabama
Attn: CR-4803a

1 Redstone Scientific Information Center
U.S. Army Missile Command
Redstone Arsenal, Alabama

1 Electronics Research Laboratory
University of California
Berkeley 4, California

2 Hughes Aircraft Company
Florence and Teale
Culver City, California
Attn: M.E. Devereux
Technical Document Center

3 Autonetics
9150 East Imperial Highway
Downey, California
Attn: Tech. Library, 3041-11

1 Dr. Arnold T. Nordsieck
General Motors Corporation
Defense Research Laboratories
6767 Hollister Avenue
Goleta, California

1 University of California
Lawrence Radiation Laboratory
P.O. Box 808
Livermore, California

1 Mr. Thomas L. Hartwick
Aerospace Corporation
P.O. Box 95085
Los Angeles 45, California

1 Professor Zorab Kaprelian
University of Southern California
University Park
Los Angeles 7, California

1 Sylvania Electronic Systems-West
Electronic Defense Laboratories
P.O. Box 205
Mountain View, California
Attn: Documents Center

1 Varian Associates
611 Hansen Way
Palo Alto, California 94303
Attn: Technical Library

1 Huston Denslow
Library Supervisor
Jet Propulsion Laboratory
California Institute of Technology
Pasadena, California

1 Professor Nicholas George
California Institute of Technology
Electrical Engineering Department
Pasadena, California

1 Space Technology Labs., Inc.
One Space Park
Redondo Beach, California
Attn: Acquisitions Group
STL Technical Library

2 Commanding Officer and Director
U.S. Navy Electronics Laboratory
San Diego, California 92052
Attn: Code 2800, C.S. Manning

1 Commanding Officer and Director
U.S. Navy Electronics Laboratory
San Diego, California 92052

1 Commanding Officer
Office of Naval Research Branch Office
1000 Geary Street
San Francisco, California 94109

1 The RAND Corporation
1700 Main Street
Santa Monica, California
Attn: Library

1 Stanford Electronics Laboratories
Stanford University
Stanford, California
Attn: SEL Documents Librarian

1 Dr. L.F. Carter
Chief Scientist Air Force
Room 4E-324, Pentagon
Washington 25, D.C.

1 Mr. Robert L. Feik
Associate Director for Research
Research and Technology Division
AFSC
Bolling Air Force Base 25, D.C.

1 Captain Paul Johnson (USN-Ret)
National Aeronautics and Space
Administration
1520 H. Street, N.W.
Washington 25, D.C.

1 Major Edwin H. Myers
Headquarters USAF (AFRDR)
Washington 25, D.C.

1 Dr. James Ward
Office of Deputy Director
(Research and Info)
Department of Defense
Washington 25, D.C.

1 Dr. Alan T. Waterman
Director, National Science Foundation
Washington 25, D.C.

1 Mr. G.D. Watson
Defense Research Member
Canadian Joint Staff
2450 Massachusetts Ave., N.W.
Washington 8, D.C.

1 Mr. Arthur G. Wimer
Chief Scientist
Air Force Systems Command
Andrews Air Force Base
Washington 25, D.C.

1 Director Advanced Research
Projects Agency
Washington 25, D.C.

1 Air Force Office of Scientific Research
Directorate of Engineering Sciences
Washington 25, D.C.
Attn: Electronics Division

1 Director of Science and Technology
Headquarters, USAF
Washington 25, D.C.
Attn: AFRST-EL/GU

1 AFRST - SC
Headquarters, USAF
Washington 25, D.C.

1 Headquarters, R & T Division
Bolling Air Force Base
Washington 25, D.C.
Attn: RTHR

1 Headquarters, U.S. Army Materiel Command
Research Division, R & D Directorate
Washington 24, D.C.
Attn: Physics and Electronics Branch
Electronics Section

1 Commanding General
U.S. Army Materiel Command
Washington 25, D.C.
Attn: R & D Directorate

1 Commanding Officer
Diamond Ordnance Fuze Laboratories
Washington 25, D.C.
Attn: Librarian, Room 211, Bldg. 92

1 Operations Evaluation Group
Chief of Naval Operations (OP-13EG)
Department of Navy
Washington, D.C. 20350

1 Chief of Naval Operations (Code OP-07T)
Department of the Navy
Washington , D.C. 20350

1 Commanding Officer
U.S. Army Personnel Research Office
Washington 25, D.C.

1 Commanding Officer & Director
Code 142 Library
David W. Taylor Model Basin
Washington, D.C. 20360

1 Chief, Bureau of Ships (Code 686)
Department of the Navy
Washington, D.C. 20360

1 Chief, Bureau of Ships (Code 732)
Department of the Navy
Washington, D.C. 20360

1 Chief, Bureau of Naval Weapons
Technical Library, DLI-3
Department of the Navy
Washington, D.C. 20360

1 Director, (Code 5140)
U.S. Naval Research Laboratory
Washington, D.C. 20390

1 Chief of Naval Research (Code 437)
Department of the Navy
Washington, D.C. 20360

1 Dr. H. Wallace Sinaiko
Institute for Defense Analyses
Research & Engineering Support Division
1666 Connecticut Ave., N.W.
Washington 9, D.C.

1 Data Processing Systems Division
National Bureau of Standards
Conn. at Van Ness
Room 239, Bldg. 10
Washington 25, D.C.
Attn: A.E. Smilow

1 National Bureau of Standards
Research Information Center &
Advisory Service on Information
Processing
Data Processing Systems Division
Washington 25, D.C.

1 Exchange and Gift Division
The Library of Congress
Washington 25, D.C.

1 NASA Headquarters
Office of Applications
400 Maryland Avenue, s.w.
Washington 25, D.C.
Attn: Mr. A.M. Greg Andrus
Code FC

1 APGC (PGAPI)
Eglin Air Force Base
Florida

1 Martin Company
P.O. Box 5837
Orlando, Florida
Attn: Engineering Library
MP-30

1 Commanding Officer
Office of Naval Research, Branch Office
230 North Michigan
Chicago , Illinois 60601

1 Laboratories for Applied Sciences
University of Chicago
6220 South Drexel
Chicago, Illinois 60637

1 Librarian
School of Electrical Engineering
Purdue University
Lafayette, Indiana

1 Donald L. Epley
Department of Electrical Engineering
State University of Iowa
Iowa City, Iowa

1 Commanding Officer
U.S. Army Medical Research Laboratory
Fort Knox, Kentucky

2 Keats A. Pullen, JR.
Ballistic Research Laboratories
Aberdeen Proving Ground, Maryland

1 Director
U.S. Army Human Engineering Laboratories
Aberdeen Proving Ground, Maryland

1 Mr. James Tippett
National Security Agency
Fort Meade, Maryland

1 Commander
Air Force Cambridge Research Laboratories
Laurence G. Hanscom Field
Bedford, Massachusetts

1 Dr. Lloyd Hollingsworth
Director, ESD AFCRL
L.G. Hanscom Field
Bedford, Massachusetts

1 Data Sciences Laboratory
Air Force Cambridge Research Lab.
Office of Aerospace Research, USAF
L.G. Hanscom Field
Bedford, Massachusetts
Attn: Lt. Stephen J. Kahne - CRB

1 Instrumentation Laboratory
Massachusetts Institute of Technology
68 Albany Street
Cambridge 39, Massachusetts
Attn: Library W1-109

1 Research Laboratory of Electronics
Massachusetts Institute of Technology
Cambridge 39, Massachusetts
Attn: Document Room 26-327

1 Dr. Robert Kingston
Lincoln Laboratories
Lexington, Massachusetts

1 Lincoln Laboratory
Massachusetts Institute of Technology
P.O. Box 73
Lexington 73, Massachusetts
Attn: Library, A-082

1 Sylvania Electric Products, Inc.
Electronic Systems
Waltham Labs. Library
100 First Avenue
Waltham 54, Massachusetts

1 Minneapolis-Honeywell Regulator Co.
Aeronautical Division
2600 Ridgeway Road
Minneapolis 13, Minnesota
Attn: Dr. D.F. Elwell
Main Station : 625

1 Inspector of Naval Material
Bureau of Ships Technical Representative
1902 West Minnehaha Avenue
St. Paul 4, Minnesota

20 Activity Supply Officer, USAELRDL
Building 2504, Charles Wood Area
Fort Monmouth, New Jersey
For: Accountable Property Officer
Marked: For Inst. for Exploratory Research
Inspect at Destination
Order No. 576-PM-63-91

1 Commanding General
U.S. Army Electronic Command
Fort Monmouth, New Jersey
Attn: AMSEL-RE

1 Miss F. Cloak
Radio Corporation of America
RCA Laboratories
David Sarnoff Research Center
Princeton, New Jersey

1 Mr. A.A. Lundstrom
Bell Telephone Laboratories
Room 2E-127
Whippany Road
Whippany, New Jersey

1 AFMDC (MDSGO Maj. P. Wheeler, Jr.)
Holloman Air Force Base
New Mexico 88330

1 Commanding General
White Sands Missile Range
New Mexico

1 Microwave Research Institute
Polytechnic Institute of Brooklyn
55 John Street
Brooklyn 1, New York

1 Cornell Aeronautical Laboratory, Inc.
4455 Genesee Street
Buffalo 21, New York
Attn: J.P. Desmond, Librarian

1 Sperry Gyroscope Company
Marine Division Library
155 Glen Cove Road
Carle Place, L.I., New York
Attn; Mrs. Barbara Judd

1 Major William Harris
RADC (RAWI)
Griffiss Air Force Base
New York

1 Rome Air Development Center
Griffiss Air Force Base
New York
Attn: Documents Library
RAALD

1 Library
Light Military Electronics Department
General Electric Company
Armament & Control Products Section
Johnson City, New York

1 Columbia Radiation Laboratory
Columbia University
538 West 120th Street
New York 57, New York

1 Mr. Alan Barnum
Rome Air Development Center
Griffiss Air Force Base
Rome, New York

1 Dr. E. Howard Holt
Director
Plasma Research Laboratory
Rensselaer Polytechnic Institute
Troy, New York

3 Commanding Officer
U.S. Army Research Office (Durham)
Box CM, Duke Station
Durham, North Carolina
Attn: CRD-AA-IP, Mr. Ulsh

1 Battelle-DEFENDER
Battelle Memorial Institute
505 King Avenue
Columbus 1, Ohio

1 Aeronautical Systems Division
Navigation and Guidance Laboratory
Wright-Patterson Air Force Base
Ohio

1 Aeronautical Systems Division
Directorate of Systems Dynamic Analysis
Wright-Patterson Air Force Base
Ohio

1 Commander
Research & Technology Div.
Wright-Patterson Air Force Base
Ohio 45433
Attn: MAYT (Mr. Evans)

1 Commanding Officer (AD-5)
U.S. Naval Air Development Center
Johnsville, Pennsylvania
Attn: NADC Library

2 Commanding Officer
Frankford Arsenal
Philadelphia 37, Pennsylvania
Attn: SMUFA-1300

1 H.E. Cochran
Oak Ridge National Laboratory
P.O. Box X
Oak Ridge, Tennessee

1 U.S. Atomic Energy Commission
Office of Technical Information Extension
P.O. Box 62
Oak Ridge, Tennessee

1 President
U.S. Army Air Defense Board
Fort Bliss, Texas

1 Director
Human Resources Research Office
The George Washington University
300 North Washington Street
Alexandria, Virginia

20 Defense Documentation Center
for Scientific & Technical Information
Cameron Station
Alexandria, Virginia 22314

1 Commander
U.S. Army Research Office
Highland Building
3045 Columbia Pike
Arlington 4, Virginia

1 U.S. Naval Weapons Laboratory
Computation and Analysis Laboratory
Dahlgren, Virginia
Attn: Mr. Ralph A. Niemann